CrossMark

Therapeutic Potential of DNAzyme Loaded on Chitosan/Cyclodextrin Nanoparticle to Recovery of Chemosensitivity in the MCF-7 Cell Line

Elham Zokaei[1] · Arastoo Badoei-dalfrad[1] ·
Mehdi Ansari[2] · Zahra Karami[1] · Touba Eslaminejad[3] ·
Seyed Noureddin Nematollahi-Mahani[4]

Abstract Commonly, acquired resistances to anticancer drug are mediated by overexpression of a membrane-associated protein that encode via multi-drug resistance gene-1 (MDR1). Herein, the mRNA-cleaving DNAzyme that targets the mRNA of MDR1 gene in doxorubicin-resistant breast cancer cell line (MCF-7/DR) loaded on the chitosan β-cyclodextrin complexes was used as a tropical agent. Chitosan/β-cyclodextrin complexes were used to deliver DNAzymes into cancer cells. Determination of the physicochemical characteristics of the particles was done by photon correlation spectroscopy and scanning electron microscopy. The encapsulation efficiency of the complexes was tested by using gel retardation assay. Positively charged nanoparticles interacted with DNAzyme that could perform as an efficient DNAzyme transfection system. The rationale usage of this platform is to sensitize MCF-7/DR to doxorubicin by downregulating the drug-resistance gene MDR1. Results demonstrated a downregulation of MDR1 mRNAs in MCF-7/DR/DNZ by real-time PCR, compared to the MCF-7/DR as control. WST1 assay showed the 22-fold decrease in drug resistance on treated cells 24 h after transfection. Results showed the intracellular accumulation of Rh123 increased in the treated cells with DNAzyme. Results suggested a potential platform in association with chemotherapy drug for cancer therapy and indicated extremely efficient at delivery of DNAzyme in restoring chemosensitivity.

✉ Arastoo Badoei-dalfrad
  badoei@uk.ac.ir

✉ Mehdi Ansari
  mansari@kmu.ac.ir

[1] Department of Biology, Faculty of Sciences, Shahid Bahonar University of Kerman, Kerman, Iran

[2] Pharmaceutics Research Centre, Faculty of Pharmacy, Kerman University of Medical Sciences, Haft-Bagh Boulevard, PO Box 76175-439, Kerman 7616931555, Iran

[3] Department of Anatomy, Afzalipour School of Medicine, Kerman University of Medical Sciences, Kerman, Iran

[4] Pharmaceutics Research Centre, Institute of Neuropharmacology, Kerman University of Medical Sciences, Kerman, Iran

🙋 Springer

Introduction

Chemotherapy is one of the mainstream anticancer therapies and has been the most popular strategy due to the simplicity of the administration of the medication, although the prolong usage of it leads to the incidence of dependent side effects and drug resistance [1, 2]. Multiple drug resistance (MDR) is caused due to the insensitivity of the cancer cells to drug and treatment failure [3]. One of the basic mechanisms of MDR versus a wide range of anticancers is the overexpression of ATP-dependent transporter to the large family of ABC membrane transporter (P-glycoprotein). This membrane efflux pumps can flush out the chemotherapeutic drugs and therefore decrease intracellular drug concentration and efficiency [4, 5]. Chemical drugs and gene therapy methods such as antisense technology like small interfering RNA (siRNA) [6, 7], antisense oligonucleotides (ASOs) [8], ribozymes, and DNAzyme (DNZ) [9] as of the main strategies have been used to overcome the MDR phenotype and as anticancer agents [10]. One of the new and more efficient ribonucleic acid catalytic methods is DNZ that selected through *SELEX*, which showed the higher efficiency, lower toxicity, and faster and more lasting effect compared to others [11, 12]. DNAzyme takes part in a diversity of fields and applications. For example, they work as the molecular recognition component in biosensors, and those with peroxidase-like activity have therapeutic applications and are also able to detect miRNAs and heavy metals [Mg^{2+}, Cu^{2+}, Pb^{2+}, Hg^{2+}, etc.] and metabolite such as choline [13, 14]. The most common studied DNZs are 10–23 and 8–17 nucleotides, which both cleaving the mRNA and require metal ions like Mg^{2+} for their activity. 10–23 nucleotide DNZ that was designed as early as in 2003 [15] has a catalytic domain of 15 deoxyribonucleotides and two substrate-binding arms of 7–9 deoxyribonucleotides. This DNZ effectively cleaves the substrate RNA at unpaired purine and paired pyrimidine (R–Y, R=A or G; Y=U or C) dinucleotides easily in a chemical system and is the best-understood model in therapeutic applications due to its simpler design and higher catalytic power [12, 15–17]. There are a few studies of DNZ on reversal of drug resistance in breast cancer, which were compared to ASODN and ribozymes targeted to the same region [9, 18]. Although developing this technology proved to be potential agents in knocking down the gene expression, their effective delivery to the targeted sites into the cell remains a challenging hurdle [19, 20]. The success of gene therapy is largely depends on the development of a carrier that can act selectively and efficiently. Delivering a gene to the targeted cells with minimal toxicity is achieved by gene condensation with cationic polymer (chitosan) and lipids (liposomes) [19, 21].

Chitosan (CS) is a better carrier for drug delivery due to its loading capacity, biocompatibility, biodegradability, low toxicity, mucoadhesiveness, and considerably inexpensive polysaccharide [22–24]. Preparation of chitosan nanoparticles was done via a technique based on ionic gelation by applying sodium tripolyphosphate (TPP) as a cross-linking agent that improves the capacity of nanoparticles [25, 26].

A novel generation of polysaccharide nanocarriers was reported which consists of the polysaccharide CS and oligosaccharides cyclodextrins (CDs) [27]. The backup logic of these designed nanocarriers was to combine the behavior of developed promising of CS nanoparticles with the outstanding biopharmaceutical features of CD [28]. Actually CDs are very common to the delivering of the genes, since their capability to enhance membrane permeability protects drugs from physical, chemical, and enzymatic degradation [29].

Various formulations of chitosan/cyclodextrin nanoparticles have been known. They have been used to deliver hydrophobic small molecules such as curcumin or doxorubicin [30] and macromolecule such as insulin and heparin [28]. In addition, they were also used for delivery of small peptides like glutathione [31]. The nanoparticle complex such as CS/CD/TPP has been also used as small molecule drug carrier [32], as well as the potential of this nanoparticles was assessed as a vehicle for delivery of genes [33]. In 2016, they were used as a potential carrier for pmCherry-C1 gene delivery, and their transfection efficiency was compared to that of lipofectamine and electroporation [34]. The aim of this study was to use CS/CD/TPP nanoparticle complex (made of chitosan, TPP, and β-cyclodextrin) for delivery of DNAzyme targeting mRNA of MDR1 on the breast carcinoma cells (MCF-7/DR) that were resistance by drug.

Materials and Methods

Chemicals

Low molecular weight chitosan (CS) and β-cyclodextrin (CD) were purchased from FMC Biopolymers (Norway). The oligonucleotides (DNAzyme) were made by Bioneer Corporation (South Korea). Dulbecco's modified Eagle medium (DMEM) and fetal bovine serum (FBS) were purchased from Gibco™ (UK). Penicillin/streptomycin (100 mg/mL), phosphate-buffered saline (PBS), water soluble tetrazolium salt 1 (WST1), rhodamine 123, and pentasodium tripolyphosphate (TPP) were all obtained by Sigma–Aldrich (Saint-Quentin Fallavier, France). DNA ladder (50 bp) was received from Biolabs (England). Triton X-100 and DMSO were obtained from Fluka Biochem (France). All other materials were of the greatest grade commercially available.

Cell Culture and Drug Treatment

The human breast carcinoma cell line (MCF-7), which was sensitive to Dox, was obtained from the Pasteur institute. The MCF-7 cells were maintained in DMEM medium containing 10% (v/v) FBS and 100 units/mL penicillin/streptomycin. Cells were incubated at 37 °C, 5% CO_2 and 90% humidified incubator used. Dox (2 mg/mL) was used to develop MCF-7/DR$_{640}$ (DR$_{640}$: Dox resistance at 640 nM final concentration) cell line resistance by stepwise selection of parental cells after six steps increasing concentrations of Dox [35]. Cell viability was determined by using WST-1 cell proliferation assay [36]. Briefly, 10^4 cells were seeded on each well into a 96-well plate and incubated overnight. In the next day, cells were treated by different doses of Dox and incubated for 24 h in the incubator conditions. After that, 10 μL of the WST-1 was added to each well and incubated for 4 h in the incubator, and then, the absorbance was read by ELISA microplate reader (BioTek_Elx800) at 420 nm. The viability percent of the cells was calculated by using the following equation:

$$\text{Cell viability}(\%) = (\text{OD420 treatment}/\text{OD420 control}) \times 100$$

Investigation of the Intracellular Doxorubicin Accumulation

The distribution of intracellular Dox within MCF-7 and MCF-7/DR$_{640}$ cells was analyzed based on the inherent fluorescence. Cells were incubated in 5 mM Dox for 2 h at 37 °C and then washed with cold PBS buffer while observing under a fluorescence microscope at a magnification of 100 μM. The absorption and emission wavelengths of Dox are 575 and 488 nm, respectively [35].

DNAzyme Preparation

According to Goa et al. [18], 12 accessible sites of purine-pyrimidine dinucleotides were identified on the secondary structure surface of the MDR1 mRNA and 12 DNZs were designed by using a computer RNA secondary structure analysis program (m-fold 3.2). In conformity with chemosensitivity assay, anti-MDR1 DNZ at targeting translation initiation codon AUG is the best one at reversing the MDR phenotype in MCF-7/DR cells. We used this sequence to knock out MDR1 mRNA expression (Fig. 1). We also use three phosphorothioate (PS) linkages that incorporated into each of the arms in DNZ.

Preparation of the Nanoparticle Complex

Chitosan nanoparticles were prepared by the ionic gelation method using TPP as a cross-linking and β-cyclodextrin as a copolymer to increase transfection efficiency and stability against enzymatic degradation with low in vitro and in vivo toxicity and improved biopharmaceutical properties of chitosan [27].

The solutions of CD with TPP and DNZ were mixed dropwise into the CS under agitation to allow complete formation of system. CS acidic solution (1.0% glacial acetic acid) was prepared at a concentration of 0.2 mg/mL. The corresponding volumes of the CD aqueous solution (0.6–1.2 mg/mL) and TPP solution (0.15 mg/mL) were mixed at a final volume of 300 μL. To encapsulate DNZ into complex nanoparticle, the required amount of the DNZ was incorporated directly into the CD/TPP phase. The DNZ/CD/TPP solution was added dropwise under constant stirring to the 1 mL of the chitosan (CS) solution at N/P ratios 3.5 and incubated at room temperature for 30 min.
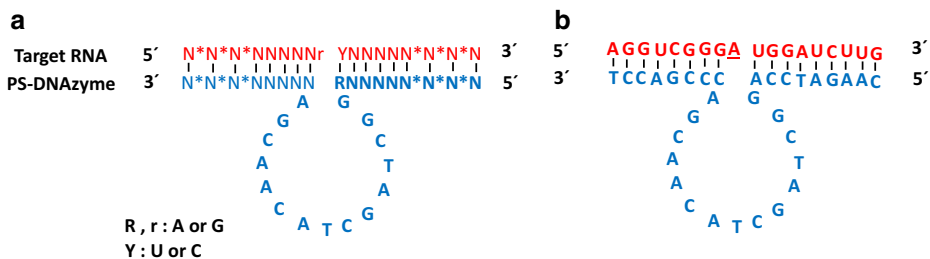

Fig. 1 Schematic structure and explanation of "10–23" DNZ. **a** Phosphorothioate-modified DNZ (PS-DNAzyme) as displayed via asterisk. DNZ annealed to the MDR1 mRNA substrate. **b** The sequences of DNZ and MDR1 mRNA. Phosphorothioate DNZ targeting between the A and U nucleotides (AUG) in translation initiation codon and cleavage this site

Characterization of Synthesized Nanoparticles

The particle size and size distribution of the CS/CD/TPP complex were determined by photon correlation spectroscopy (PCS) and laser Doppler anemometry (LDA) using a zeta potential nano ZS. The size, surface, and cross-sectional morphology of the chitosan nanoparticles (sonicated) were observed by scanning electron microscopy (SEM, DSM-960A) after sputter coating with gold for 5 min. All samples were examined at an acceleration voltage of 15 kV. Gel retardation assay of the complexes CS/CD/TPP/DNZ was done by using electrophoresis on 1.5% agarose gel, running at 100 V for 30 min [37].

Transfection Study

Cells were seeded in a 96-well plate at a density of 6×10^3 cells/well in 100 μL of free serum medium. After 24 h, the cells were transfected with the CS/CD/TPP/DNZ complexes at differing DNZ concentration of 0.5–6.0 μg/mL. Chemosensitivity assay analyses were done after 24–72 h.

Determination of MDR1 mRNA Levels

Total RNA was extracted by using TRIzol® reagent following the manufacturer's instructions. After 24-h post-transfection with DNZ and unspecific DNZ, four groups of cells (MCF-7 as control MCF-7/DR, MCF-7/DR + DNZ, MC7/DR + unspecific DNZ) were lysed by incubating in 1 mL of TRIzol® reagent. Then, cDNA synthesizing with RNA was carried out using a reverse transcriptase kit (AccuPower® CycleScript RT PreMix (dN6) kit (Bioneer)) in 20 μL of final volume. RT-qPCR was performed using the green master reaction mix with lowROX (Jena Bioscience) in a Rotor-gene real-time PCR system, using 1 μL of each cDNA sample and 10 pmol of each primer as shown in Table 1. All reactions were run in triplicate. Threshold cycle (CT) data were collected and average ΔCT of each group was calculated as follows: ΔCT = average CT_{MDR1} − average CT_{GAPDH}. ΔCT was defined as relative MDR1 mRNA expression level and used for analysis. The difference of the relative MDR1 mRNA expression between MDR cancer cells and the treated groups was calculating using the $2^{-\Delta\Delta CT}$ method ($\Delta\Delta$CT = ΔCT of treated group − ΔCT of control group) [9, 18].

Rhodamine 123 Accumulation *Assay* (Rh123)

Rh123 accumulation assay determined P-GP activity by comparing intracellular accumulation of Rh123 in MCF-7/DR$_{640}$ and MCF-7 in the absence or presence of DNZ as P-GP inhibitors.

Table 1 Oligonucleotide primers were used in this study

Oligonucleotide	Primer sequence [5′ → 3′]	Amplicon size (bp)
MDR1	F: CGCCAAGCCATGTTTCTGTT	102
	R: CATAGAAAGGAAATGATTCAGCTCT	
*GAPDH	F: TGCACCACCAACTGCTTAGC	87
	R: GGCATGGACTGTGGTCATGAG	
DNAzyme	TCCAGCCCAGCAACATCGATCGGACCTAGAAC	32
Unspecific DNAzyme	TCAGGATCAGCAACATCGATCGGCGCATGGCG	32

*Housekeeping gene

Initially, 10^4 cells were seeded in 96-well plate and allowed to reach 80% fluency, and then, cells were incubated with 5 μM Rh123 at 37 °C for 30 min. Then, the Rh123 medium was replaced with complete medium (10% FBS) and incubated at 37 °C for 45 min. Cells were washed three times in cold phosphate-buffered saline and lysed by Triton X-100. The intracellular levels of Rh123 were quantified by microplate fluorescence reader (BioTek ELx808) at 485 nm with reference 535 nm [38]. All analyses were performed in three times in the triplicate.

Cell Proliferation Assay

Cell cytotoxicity was measured by seeded cells in 96-well plate, which were transfected by different concentrations of DNZ ranged from 0.5–6.0 μg/mL. The absorbance of untreated controls was taken as 100% survival, and the percentage of cell survival rate is evaluated as 100 (treated cells − blank)/(untreated cells − blank), and growth inhibition is defined as 100 − cell survival rate (%) (blank is medium without cells + WST1 + solubilizing buffer). The value of relative drug resistance was calculated using the following *formula*: the IC50 of treated cells/the IC50 of untreated MCF-7 cells [9, 18].

IC50 is the drug concentration of the drug that causes 50% inhibition of the desired activity. The reversal fold was determined by following *formula*: the IC50 for anticancer drugs/the IC50 for anticancer drugs plus DNZ in resistance cells. All experiments were performed in triplicate.

Statistical Analysis

All statistical analyses were performed using IBM SPSS statistics version 21 software. The normal distribution were presented as means ± SEM. Each experiment was repeated three times. Statistical differences were performed by one-way analysis of variance (ANOVA) followed by the appropriate post-test as described in the figure legends. A $p \leq 0.05$ was considered statistically significant.

Results

Dox-Resistant Cells

Evaluation of Dox-Resistant Cells

Based on the cytotoxicity test, the relative drug resistance of MCF-7/DR$_{640}$ was compared with the control in the presence of different concentrations of Dox (Fig. 2). The cells exhibited significant resistance to the corresponding drug. The IC$_{50}$ values for MCF-7 and MCF-7/DR$_{640}$ were 0.202 and 16.74 μM, respectively. MCF-7/DR$_{640}$ was considerably less sensitive to Dox than MCF-7 at different concentrations with a maximum 82-fold increase in resistance.

Morphological Characteristics

Morphologically resistance cells were evaluated. Resistant cells were larger in size, more irregular, rounded shape, and multi-nuclei compared to the normal cells. Multiple vesicles were also observed in the cytoplasm and increased cell adhesion to cell and to the floor of the flask. The morphological characteristics of the resistant and normal cells are shown in Fig. 3.
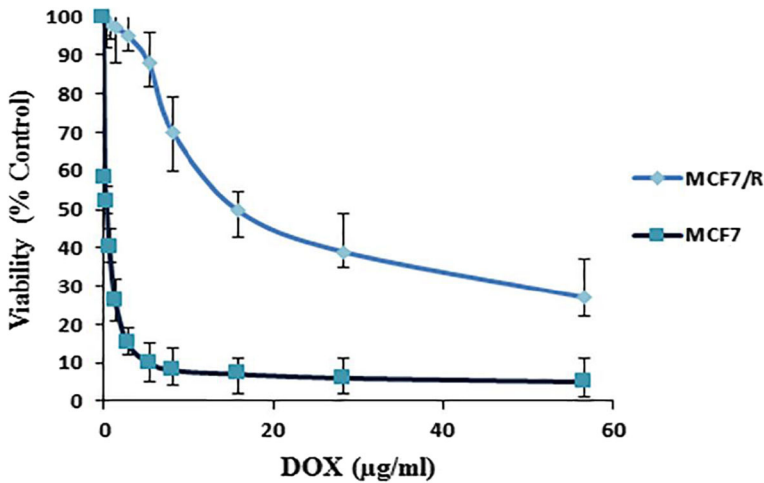
Fig. 2 The curves of comparison of the MCF-7/DR$_{640}$ and MCF-7 response to Dox

Evaluation of the Intracellular Dox Accumulation

The accumulation and localization of intracellular Dox in MCF-7 and MCF-7/DR$_{640}$ cells were determined by using fluorescence microscopy (Fig. 4). The results showed that Dox was specifically concentrated in the nucleus of the MCF-7 cells as the control while MCF-7/DR$_{640}$ cells showed no clear fluorescence in their nucleus. Instead, multiple fluorescence vesicles have been observed in the cytoplasm of resistant cells, which were preferably around the nucleus.

Characterization of Nanoparticles

The morphology and distribution of chitosan complex were further characterized by SEM. The SEM micrographs of CS/CD/TPP complex are shown in Fig. 5. The particle size of CS/CD/TPP complex was approximately 200 ± 14 nm. Macroscopically nanoparticles appeared as a long chain of interacting particles which were composed of small nanoparticles.
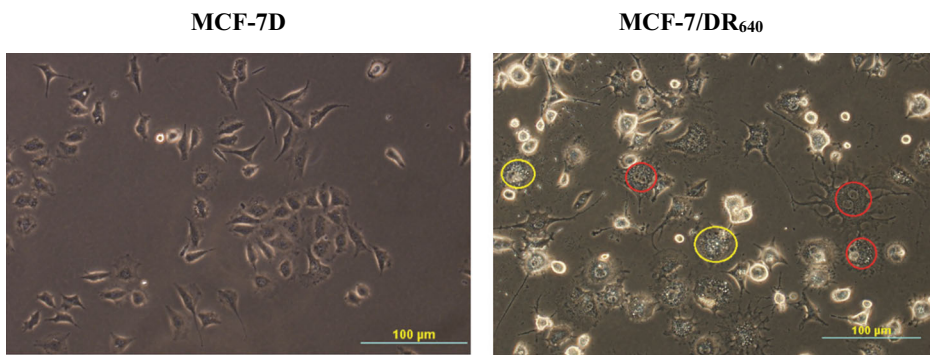
MCF-7D   **MCF-7/DR$_{640}$**

Fig. 3 MCF-7 and MCF-7/DR$_{640}$ cell morphology. Parental cells are regular and spindle shaped while MCF-7/DR$_{640}$ cells emerge irregular, multi-nuclei (marked in red circles) and vesicles containing Dox (marked in yellow circles)
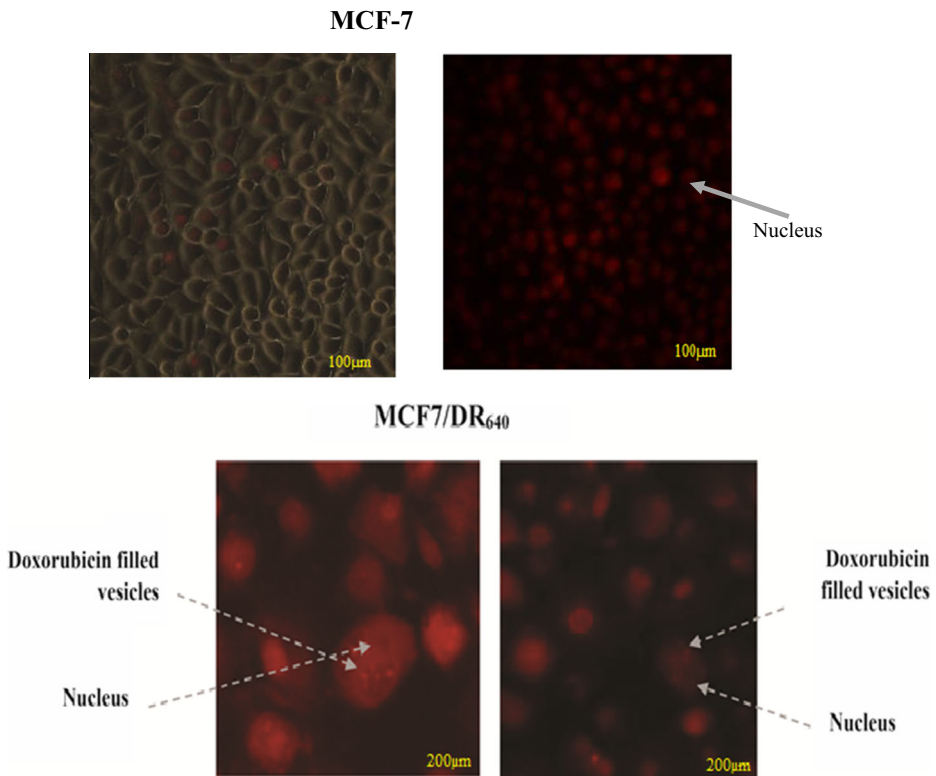
MCF-7

Nucleus

100μm

100μm

MCF7/DR$_{640}$

Doxorubicin filled vesicles

Nucleus

200μm

Doxorubicin filled vesicles

Nucleus

200μm

Fig. 4 The accumulation and localization of intracellular Dox in MCF-7 and MCF-7/DR$_{640}$ cells. The nuclei of MCF-7 cells show high fluorescence light compared with cellular nucleus of MCF-7/DR$_{640}$, and vesicles containing Dox are seen in the cytoplasm

Gel retardation assay showed that nanoparticles and DNZ were bounded tightly and completely in N/P ratio 3.5. Nanoparticles that showed a low fluorescence in the well suggested the formation of adducts and, in correspondence to the free DNZ band, suggested that DNZ might be partially bounded on the surface of the nanoparticle (Fig. 6). The average diameters of particle complex were 244.2 nm measured by DLS and did not increase after 12-week storage at 4 °C. The zeta potential of CS/CD/TPP was − 6.48.

MDR1 Gene Expression

Results showed that the delivery of DNZ by nanoparticles in Dox-resistant cells decreased the expression of MDR1 to 5.2 folds compared to the untreated MCF-7/DR$_{640}$ with DNZ (Fig. 7).

Determination of P-GP Function

Intracellular Rh123 accumulation had increased in the cells that were treated with DNZ as compared to that in the untreated cells (MCF-7/DR$_{640}$ and MCF-7) which indicated P-GP expression was reduced. The amount of intracellular Rh123 in the

SEM HV: 15.0 kV | WD: 6.83 mm | 500 nm | MIRA3 TESCAN
View field: 2.77 µm | Det: SE | |
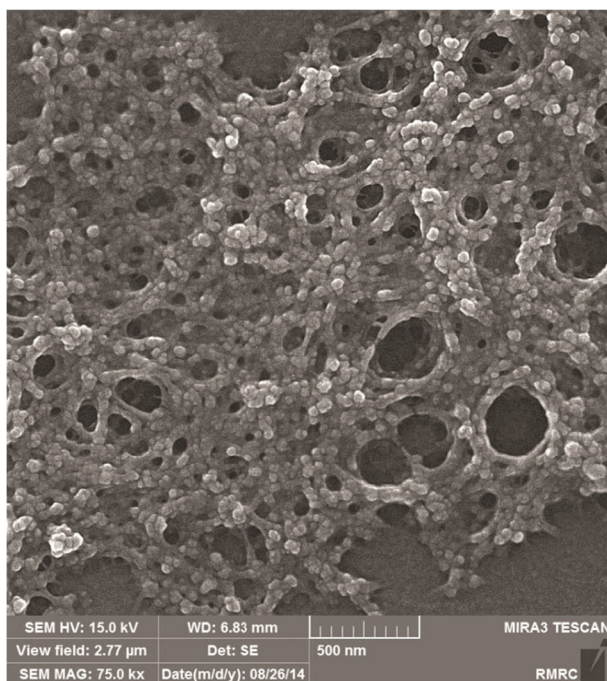SEM MAG: 75.0 kx | Date(m/d/y): 08/26/14 | | RMRC

Fig. 5 SEM micrographs of nanoparticle complex (scales 500 nm, 2 lm)

resistant cells compared to that in MCF-7 cells decreased about 4.7 folds and, after transfection with CS/CD/TPP/DNZ combination, increased about 2.6 folds. This experiment was carried out 24 h after transfection (Fig. 8).

Fig. 6 Gel retardation assay of the nanoparticles encapsulating DNZ. Lane 1: marker; 2: DNZ; 3: fresh complex of nanoparticle and DNZ at N/P ratio of 3.5; 4: complex of nanoparticle and DNZ after 3 months
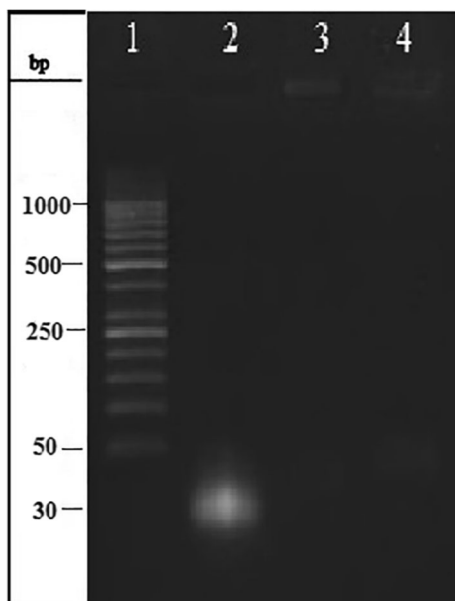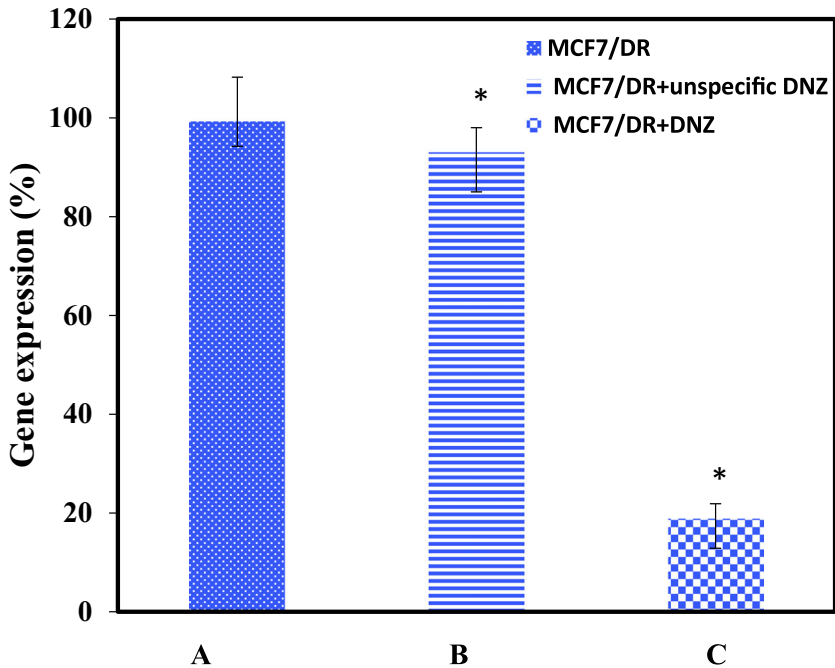
Fig. 7 Comparison of MDR1 gene expression in treated and untreated MCF-7/DR_{640} cells with DNZ and unspecific DNZ. mRNA level for MDR1 in MCF-7 cells was measured by RT-qPCR. (A) The expression of MDR1 mRNA in MCF7/DR_{640}, (B) the expression of MDR1 mRNA in MCF7/DR_{640} treated by unspecific DNZ, and (C) the expression of MDR1 mRNA in MCF7/DR_{640} treated by DNZ. MCF-7 was used as control
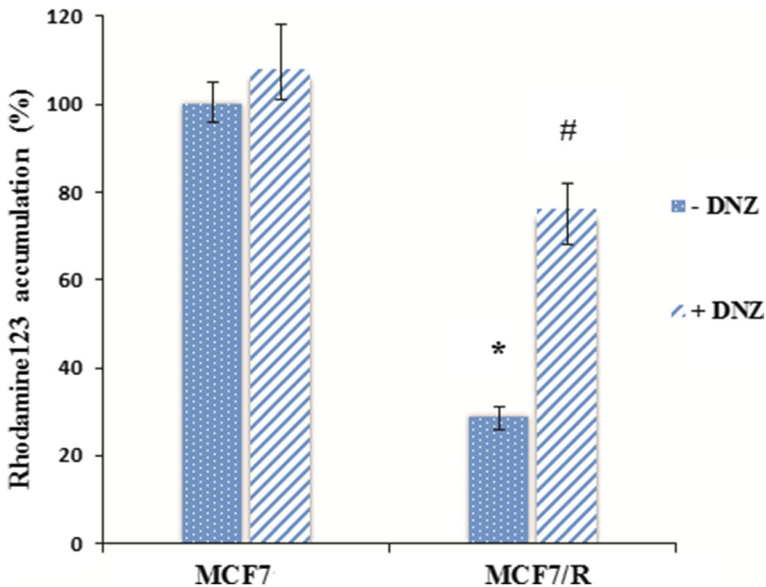

Fig. 8 Accumulation of Rh123 in treated and untreated two types of cells (MCF-7 and MCF-7/DR_{640}) via DNZ. According to data, cells treated with DNZ showed higher fluorescent due to inhibition of drug resistance. *$p < 0.05$ when compared with MCF-7 cells, #$p < 0.05$ when compared with counterparts not exposed to DNZ
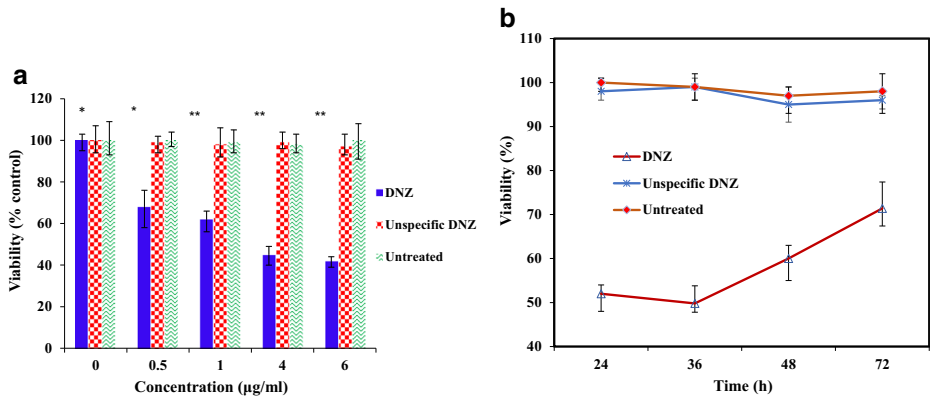
Fig. 9 **a** The MCF-7/DR$_{640}$ cells were transfected with 0.5- to 6.0-µg/mL concentrations of DNZ, in a dose-dependent response. *$p < 0.05$, **$p < 0.01$. **b** MCF-7/DR$_{640}$ cells were treated with DNZ, at a concentration of 4 µg/mL observed at 24, 36, 48, and 72 h after transfection. The suppression efficiency of DNZ was rapid and continuous that could cleavage MDR1 under 24 h after transfection and continuous to 72 h, with the best hit in 24–36 h after treatment

Evaluation of Cytotoxicity

The cytotoxicity of different formulations on MCF-7, MCF-7/DR$_{640}$, and MCF-7/DR$_{640}$/DNZ with different concentrations of DNZ from 0.5 to 6 µg/mL was determined by WST1. The results showed that DNZ in the dose-dependent response could reduce drug resistance on cells; furthermore, no changes were observed in the scramble DNZ groups (Fig. 9a). In the next step, the experiment was conducted 24, 36, 48, and 72 h after transfection with DNZ. The suppressive effect of DNZ was rapid and constant. It could overcome multi-drug resistance 24 h after transfection and its effects continuous for 72 h. Results showed that 22-fold reduction in drug resistancethe was obtained after 24–36 h of transfection with a 22-fold reduction in drug resistance to Dox (Fig. 9b). The reversal efficiency of DNZ and IC$_{50}$ values in the treated and untreated cells with 4 µg/mL DNZ is listed in Table 2.

Discussion

Morphological Characteristics of Dox-Resistant Cells

MCF-7/DR cells were produced by step-wised Dox selection [39]. The results of the fluorescent microscope showed that despite that the nucleus of MCF-7 cells is full of Dox, many vesicles were seen to be filled with Dox in the cytoplasm of MCF-7/DR and more were around the nuclei. Chen et al. suggested that the resistant cells protect their DNA from drug poisoning

Table 2 Assessment of chemosensitivity in treated cells

Group	IC$_{50}$ for Dox (µM)	Relative drug resistance	Fold reduction in drug resistance
MCF-7	0.202 ± 0.08	1	
MCF-7/DR	16.74 ± 0.16	82.67	
MCF-7/DR + DNZ	0.754 ± 0.12	3.73	22.16

effect by separating Dox into these vesicles and, on the other hand, eliminating the drug from the intracellular medium [40]. Rajagopal and Simon [41] reported that these vesicles may play a role in the metabolic inactivation of Dox. It may be because of the high concentration of MRP transporters that was observed in the membranes of these vesicles. Also, Dalton and Scheper [42] have found that the MVP gene, which codes for a non-ATP-dependent intra-cell pump called LRP, is responsible for the drug flow from the nucleus to the outside and may reduce the accumulation of Dox in the nucleus of MCF-7/DR. As previously mentioned, overexpression of MDR1 is one of the basic mechanisms of resistance versus a wide range of anticancer drug [4]. Thus, the delivery of anti-MDR1 DNZ to MCF-7 cells was used to the inhibition of drug resistance.

DNAzyme Preparation and Its Challenges to Restoration of Chemosensitivity

Compared to RNA, DNZ due to the structure of DNA is relatively easy to synthesize and holds great promise for diagnostic and therapeutic applications. Goa et al. [18] by comparing reversal efficiency of DNZ with other nucleic acid-based RNA showed that DNZ at 0.5 μg/mL could effectively suppress expression of MDR1 mRNA and inhibit synthesis of Pgp, with a tenfold reduction in concentration as compared to that of ASODN and anti-miR-27a inhibitor (5 μg/mL). At the same concentration, the suppressive effect of DNZ was significantly better and longer than that of ASODN and anti-miR-27a inhibitor. According to Xing et al. [8], reversal efficiency of DNZ targeting translation initiation codon AUG in breast cancer and leukemia is much better than that of other RNA-based nucleic acids targeting the same region of MDR1 mRNA, and it could reduce the mRNA MDR1 expression about 20% more than ribozyme and 38% more than ASODN, although previously investigations have shown the inhibitory effect of ribozyme and ASODN to reverse MDR in leukemia [4], colon cancer [43], and breast cancer [8].

However, use of RNA-cleaving DNZs is generally a multi-step process. The first step is screening of the accessible sites for DNZs against the target mRNA by RNA structure analysis software [44, 45]. Goe et al. [18] used these techniques for designing effective DNA enzymes that targeting translation initiation codon AUG MDR1 gene and this DNZ used in this project (Fig. 1). The second step is the improvement of the DNZ properties such as increasing its intracellular stability. To solve this challenge, 1–5 phosphorothioate (PS) linkages were incorporated into each of the arms in DNZ [46]. This modification can protect the DNZ against the action of endonucleases, promote the half-life of DNA enzyme, enhance the interaction of serum protein with DNZ, and help in better distribution. These modifications also exhibit high specificity and good binding affinity [47]. However, this linkage causes cytotoxicity via binding of phosphorothioates with various proteins. It can also increase the negative charge on the helix, and then, it decreases the binding affinity of DNZ with target mRNA, thus reducing its catalytic potency, which results from including the membrane-binding proteins [48]. So two phosphorothioate modifications are usually considered enough to provide sufficient nuclease resistance. The third challenge to the success of gene therapy is to create safe and efficient gene delivery carriers to improve biological distribution and subsequently increase cellular absorption, specificity, and also stability [49].

Transfection Efficiency of the DNAzyme to the Doxorubicin-Resistant Cells by Chitosan/Cyclodextrin Nanoparticles

Preparation of chitosan nanoparticles was facilitated by a technique based on forming via ionic gelatin with adding TPP as cross-linking agent which has been reported previously by our group

[50]. Chitosan–TPP-DNZ nanoparticles have been found to be a better vector for DNZ delivery compared to chitosan-DNZ complexes, as an alternative encapsulated DNZ into CS/CD/TPP nanoparticles was able to associate the complexes to achieve efficient gene transfer with high capacity [50, 51]. According to Eslami et al. [34], this nanoparticle complex is an effective method for introducing the gene into the cell, since not only the transfection efficiency that acquired with an optimized naked DNZ is much easier, but also measuring the rate of gene delivery that has been reported was much higher due to its low toxicity and high flexibility. Here, we use a nanoparticle that can transfect DNZ into cells. Our findings are in agreement with the previous studies on ionic gelation process for the preparation of CS/CD/TPP nanoparticles [33, 34]. The efficiency of this system for controlling DNZ on drug-resistant breast cancer cells (MCF-7/DR) has been investigated. The results showed that CS/CD/TPP nanoparticles are nontoxic and hence is a suitable biocompatible gene transfer reagent. It was possible to increase the dose of the CS/CD/TPP nanoparticles for gene delivery. The zeta potential of the complex was -6.48 mV, indicating a negative charge around the particle that prevents the accumulation of particles with each other and prevents the formation of the larger particles. N/P ratios are defined as the ratios between chitosan nitrogen (N) per DNA phosphate (P), so it depends on concentration of chitosan to DNZ. Probably, the cause of negative zeta potential is the negative charges on the TPP. The average diameters determined by DLS were larger than the sizes determined by the SEM images of the corresponding samples. This was presumably because DLS gave the mean hydrodynamic diameter of the nanoparticle core surrounded by the organic and solvation layers, whereas SEM gave the diameter of nanoparticles alone in the dry state that is consistent with previous studies [52]. The results of the electrophoresis gel indicate the ability to maintain and carry high levels of DNZ in the ratio of $N/P = 3/5$, and no DNZ release in the complex has been observed. A relatively small fluorescence in the wells has showed that the potential for DNZ bonds with nanocarriers are at the complex level [34, 37].

WST1 results demonstrated that Dox associated with DNZ-MDR1 could induce cell death in resistance cell. After including of DNZ in the delivery system, results showed a 22.4-fold reduction in the drug resistance for Dox with DNZ at 4 µg/mL compared with untreated cells. Xing et al. [9] and Goe et al. [18] reported that the transfection of 5 µg/mL DNZ into the MCF-7 cells reduce the drug resistance about 21-fold, in DNZ-treated cells after 36 h. Furthermore, the best therapeutic effect was observed 24 to 36 h after transfection. DNZs restore the chemosensitivity to Dox with approximately no toxicity. Toxicities of nanoparticles alone were also evaluated, and the results were indicative of the lack of toxicity of nanocarriers. We compared the expression of MDR1 mRNA in cells that treated by DNZ and scrambled DNZ, and the results are shown in Fig. 7.

P-GP is a multi-drug flow pump (MDR) that transports a wide range of drug. Increasing the intracellular Rh123 retention in the DNZ-treated resistant cell lines was observed, in corroboration with the suppression of P-GP function [53] that seems to be the more inhibition of expression P-GP than previous studies by Xing et al. [9]. To prove the specificity of DNZ-mediated reverse of MDR1 expression, we also examined MDR1 gene expression level. These data showed a 5.2-fold reduction in MDR1 expression in the DNZ-treated cells compared to the untreated resistance groups, which is comparable with the results of previous studies that carried out by Xing et al. [9] and Goe et al. [18].

In summary, the performance of DNZ-based suppressor of MDR1 gene and the reversal of chemosensitivity through delivery of a new generation of citizen-based nanocarriers has been improved. As a rational design of this platform, our motivation was to try to improve the two previous methods. We used the chitosan/cyclodextrin/tripolyphosphate nanocarriers for the first time to deliver the DNZ, which has been a highly encapsulated drug, is cheaper and easier to prepare, and

has high transfection efficacy, more penetration, and less toxicity. We believe that this system proposed a platform for the extension of more efficient approaches for cancer treatment. Further researches including optimization of CS/CD/TPP formulation for co-delivery Dox and DNZ-based suppressors of MDR phenotype (MDR1 and BCL2 gene) and cancer suppression in vivo model will be under investigation.

Compliance with Ethical Standards

Conflict of Interest The authors declare that they have no conflicts of interest.

References

1. Zhao, J. (2016). Cancer stem cells and chemoresistance: the smartest survives the raid. *Pharmacology & Therapeutics, 160*, 145–158.
2. Huang, Y., & Sadée, W. (2006). Membrane transporters and channels in chemoresistance and -sensitivity of tumor cells. *Cancer Letters, 239*(2), 168–182.
3. Smalley, M., Piggott, L., & Clarkson, R. (2013). Breast cancer stem cells: obstacles to therapy. *Cancer Letters, 338*(1), 57–62.
4. Motomura, S., Motoji, T., Takanashi, M., Wang, Y. H., Shiozaki, H., Sugawara, I., et al. (1998). Inhibition of P-glycoprotein and recovery of drug sensitivity of human acute leukemic blast cells by multidrug resistance gene (mdr1) antisense oligonucleotides. *Blood, 91*(9), 3163–3171.
5. Gao P, Zhou G, Zhang Q, Li H, Mu K, Yuan Y, et al. (2006). Reversal MDR in breast carcinoma cells by transfection of ribozyme designed according the secondary structure of mdr1 mRNA. The Chinese Journal of Physiology, 49(2):96.
6. Du, B., & Shim, J. S. (2016). Targeting epithelial–mesenchymal transition (EMT) to overcome drug resistance in cancer. *Molecules, 21*(7), 965.
7. Ebrahimian, M., Taghavi, S., Mokhtarzadeh, A., Ramezani, M., & Hashemi, M. (2017). Co-delivery of doxorubicin encapsulated PLGA nanoparticles and Bcl-xL shRNA using alkyl-modified PEI into breast cancer cells. *Biotechnology and Applied Biochemistry, 183*(1), 126–136.
8. Thierry, A. R., & Dritschilo, A. (1992). Liposomal delivery of antisense oligodeoxynucleotides. *Annals of the New York Academy of Sciences, 660*(1), 300–302.
9. Xing, A. Y., Shi, D. B., Liu, W., Chen, X., Sun, Y. L., Wang, X., et al. (2013). Restoration of chemosensitivity in cancer cells with MDR phenotype by deoxyribozyme, compared with ribozyme. *Experimental and Molecular Pathology, 94*(3), 481–485.
10. Fokina, A. A., Stetsenko, D. A., & François, J. C. (2015). DNA enzymes as potential therapeutics: towards clinical application of 10-23 DNAzymes. *Expert Opinion on Biological Therapy, 15*(5), 689–711.
11. Sett, A., Das, S., & Bora, U. (2014). Functional nucleic-acid-based sensors for environmental monitoring. *Applied Biochemistry and Biotechnology, 174*(3), 1073–1091.
12. Xu, Z., Yang, L., Sun, L., & Cao, Y. (2012). Use of DNAzymes for cancer research and therapy. *Chinese Science Bulletin, 57*(26), 3404–3408.
13. Nikzad, N., & Karami, Z. (2018). Label-free colorimetric sensor for sensitive detection of choline based on DNAzyme-choline oxidase coupling. *International Journal of Biological Macromolecules, 115*, 1241–1248.
14. Mahdiannasser, M., & Karami, Z. (2018). An innovative paradigm of methods in microRNAs detection: highlighting DNAzymes, the illuminators. *Biosensors & Bioelectronics, 107*, 123–144.
15. Kuznetsova, M., Fokina, A., Lukin, M., Repkova, M., Venyaminova, A., & Vlassov, V. (2003). Catalytic DNA and RNA for targeting MDR1 mRNA. *Nucleosides, Nucleotides & Nucleic Acids, 22*(5–8), 1521–1523.
16. Dass, C. R., Choong, P. F., & Khachigian, L. M. (2008). DNAzyme technology and cancer therapy: cleave and let die. *Molecular Cancer Therapeutics, 7*(2), 243–251.
17. Fokina, A. A., Kuznetsova, M. A., Repkova, M. N., & Venyaminova, A. G. (2004). Two-component 10–23 DNA enzymes. *Nucleosides, Nucleotides & Nucleic Acids, 23*(6–7), 1031–1035.
18. Gao, P., Wei, J. M., Li, P. Y., Zhang, C. J., Jian, W. C., Zhang, Y. H., et al. (2011). Screening of deoxyribozyme with high reversal efficiency against multidrug resistance in breast carcinoma cells. *Journal of Cellular and Molecular Medicine, 15*(10), 2130–2138.

19. Karnati, H. K., Yalagala, R. S., Undi, R., Pasupuleti, S. R., & Gutti, R. K. (2014). Therapeutic potential of siRNA and DNAzymes in cancer. *Tumor Biology, 35*(10), 9505–9521.

20. Khan, A., Benboubetra, M., Sayyed, P. Z., Wooi Ng, K., Fox, S., Beck, G., et al. (2004). Sustained polymeric delivery of gene silencing antisense ODNs, siRNA, DNAzymes and ribozymes: in vitro and in vivo studies. *Journal of Drug Targeting, 12*(6), 393–404.

21. Lin Tan, M., Choong, P. F., & Dass, C. R. (2009). DNAzyme delivery systems: getting past first base. *Expert Opinion on Drug Delivery, 6*(2), 127–138.

22. Fokina, A. A., Chelobanov, B. P., Fujii, M., & Stetsenko, D. A. (2017). Delivery of therapeutic RNA-cleaving oligodeoxyribonucleotides (deoxyribozymes): from cell culture studies to clinical trials. *Expert Opinion on Drug Delivery, 14*(9), 1077–1089.

23. Li, G. F., Wang, J. C., Feng, X. M., Liu, Z. D., Jiang, C. Y., & Yang, J. D. (2015). Preparation and testing of quaternized chitosan nanoparticles as gene delivery vehicles. *Biotechnology and Applied Biochemistry, 175*(7), 3244–3257.

24. Alexakis T, Boadi DK, Quong D, Groboillot A, O'neill I, Poncelet D, et al. (1995). Microencapsulation of DNA within alginate microspheres and crosslinked chitosan membranes for in vivo application. Biotechnology and Applied Biochemistry 50(1):93–106.

25. Csaba, N., Köping-Höggård, M., & Alonso, M. J. (2009). Ionically crosslinked chitosan/tripolyphosphate nanoparticles for oligonucleotide and plasmid DNA delivery. *International Journal of Pharmaceutics, 382*(1), 205–214.

26. Csaba, N., Köping-Höggård, M., Fernandez-Megia, E., Novoa-Carballal, R., Riguera, R., & Alonso, M. J. (2009). Ionically crosslinked chitosan nanoparticles as gene delivery systems: effect of PEGylation degree on in vitro and in vivo gene transfer. *Journal of Biomedical Nanotechnology, 5*(2), 162–171.

27. Trapani, A., Garcia-Fuentes, M., & Alonso, M. (2008). Novel drug nanocarriers combining hydrophilic cyclodextrins and chitosan. *Nanotechnology, 19*(18), 185101.

28. Krauland, A. H., & Alonso, M. J. (2007). Chitosan/cyclodextrin nanoparticles as macromolecular drug delivery system. *International Journal of Pharmaceutics, 340*(1-2), 134–142.

29. Challa, R., Ahuja, A., Ali, J., & Khar, R. K. (2005). Cyclodextrins in drug delivery: an updated review. *AAPS PharmSciTech, 6*(2), E329–EE57.

30. Liu, Y., Zhai, Y., Han, X., Liu, X., Liu, W., Wu, C., et al. (2014). Bioadhesive chitosan-coated cyclodextrin-based superamolecular nanomicelles to enhance the oral bioavailability of doxorubicin. *Journal of Nanoparticle Research, 16*(10), 2587.

31. Trapani, A., Lopedota, A., Franco, M., Cioffi, N., Ieva, E., Garcia-Fuentes, M., et al. (2010). A comparative study of chitosan and chitosan/cyclodextrin nanoparticles as potential carriers for the oral delivery of small peptides. *European Journal of Pharmaceutics and Biopharmaceutics, 75*(1), 26–32.

32. Thanh Nguyen, H., & Goycoolea, F. M. (2017). Chitosan/cyclodextrin/TPP nanoparticles loaded with quercetin as novel bacterial quorum sensing inhibitors. *Molecules, 22*(11), 1975.

33. Teijeiro-Osorio, D., Remuñán-López, C., & Alonso, M. J. (2009). Chitosan/cyclodextrin nanoparticles can efficiently transfect the airway epithelium in vitro. *European Journal of Pharmaceutics and Biopharmaceutics, 71*(2), 257–263.

34. Eslaminejad, T., Nematollahi-Mahani, S. N., & Ansari, M. (2016). Cationic β-cyclodextrin–chitosan conjugates as potential carrier for pmCherry-C1 gene delivery. *Molecular Biotechnology, 58*(4), 287–298.

35. AbuHammad, S., & Zihlif, M. (2013). Gene expression alterations in doxorubicin resistant MCF7 breast cancer cell line. *Genomics, 101*(4), 213–220.

36. Yin, L. M., Wei, Y., Wang, Y., Xu, Y. D., & Yang, Y. Q. (2013). Long term and standard incubations of WST-1 reagent reflect the same inhibitory trend of cell viability in rat airway smooth muscle cells. *International Journal of Medical Sciences, 10*(1), 68.

37. Zhao, Q. Q., Chen, J. L., Lv, T. F., He, C. X., Tang, G. P., Liang, W. Q., et al. (2009). N/P ratio significantly influences the transfection efficiency and cytotoxicity of a polyethylenimine/chitosan/DNA complex. *Biological & Pharmaceutical Bulletin, 32*(4), 706–710.

38. Jouan, E., Le Vée, M., Mayati, A., Denizot, C., Parmentier, Y., & Fardel, O. (2016). Evaluation of P-glycoprotein inhibitory potential using a rhodamine 123 accumulation assay. *Pharmaceutics, 8*(2), 12.

39. Tsou, S. H., Chen, T. M., Hsiao, H. T., & Chen, Y. H. (2015). A critical dose of doxorubicin is required to alter the gene expression profiles in MCF-7 cells acquiring multidrug resistance. *PLoS One, 10*(1), e0116747.

40. Chen, V. Y., Posada, M. M., Zhao, L., & Rosania, G. R. (2007). Rapid doxorubicin efflux from the nucleus of drug-resistant cancer cells following extracellular drug clearance. *Pharmaceutical Research, 24*(11), 2156–2167.

41. Rajagopal, A., & Simon, S. M. (2003). Subcellular localization and activity of multidrug resistance proteins. *Molecular Biology of the Cell, 14*(8), 3389–3399.

42. Dalton, W. S., & Scheper, R. J. (1999). Lung resistance-related protein: determining its role in multidrug resistance. *Journal of the National Cancer Institute, 91*(19), 1604–1605.

43. Ramachandran, C., & Wellham, L. L. (2003). Effect of MDR1 phosphorothioate antisense oligodeoxynucleotides in multidrug-resistant human tumor cell lines and xenografts. *Anticancer Research, 23*(3B), 2681–2690.

44. Cairns, M. J., Hopkins, T. M., Witherington, C., Wang, L., & Sun, L. Q. (1999). Target site selection for an RNA-cleaving catalytic DNA. *Nature Biotechnology, 17*(5), 480–486.

45. Beale, G., Hollins, A. J., Benboubetra, M., Sohail, M., Fox, S. P., Benter, I., et al. (2003). Gene silencing nucleic acids designed by scanning arrays: anti-EGFR activity of siRNA, ribozyme and DNA enzymes targeting a single hybridization-accessible region using the same delivery system. *Journal of Drug Targeting, 11*(7), 449–456.

46. Iversen, P. O., Nicolaysen, G., & Sioud, M. (2001). DNA enzyme targeting TNF-α mRNA improves hemodynamic performance in rats with postinfarction heart failure. *American Journal of Physiology. Heart and Circulatory Physiology, 281*(5), H2211–H22H7.

47. Takahashi, H., Hamazaki, H., Habu, Y., Hayashi, M., Abe, T., Miyano-Kurosaki, N., et al. (2004). A new modified DNA enzyme that targets influenza virus A mRNA inhibits viral infection in cultured cells. *FEBS Letters, 560*(1–3), 69–74.

48. Pun, S. H., Bellocq, N. C., Cheng, J., Grubbs, B. H., Jensen, G. S., Davis, M. E., et al. (2004). Biodistribution of RNA-cleaving DNA enzyme (DNAzyme) to tumor tissue by transferrin-modified, cyclodextrin-based particles. *Cancer Biology & Therapy, 3*, 641–650.

49. Tack, F., Bakker, A., Maes, S., Dekeyser, N., Bruining, M., Elissen-Roman, C., et al. (2006). Modified poly (propylene imine) dendrimers as effective transfection agents for catalytic DNA enzymes (DNAzymes). *Journal of Drug Targeting, 14*(2), 69–86.

50. Vimal, S., Majeed, S. A., Taju, G., Nambi, K. S. N., Raj, N. S., Madan, N., et al. (2013). RETRACTED: chitosan tripolyphosphate (CS/TPP) nanoparticles: preparation, characterization and application for gene delivery in shrimp. *Acta Tropica, 128*(3), 486–493.

51. Katas, H., & Alpar, H. O. (2006). Development and characterisation of chitosan nanoparticles for siRNA delivery. *Journal of Controlled Release, 115*(2), 216–225.

52. Takechi-Haraya, Y., Tanaka, K., Tsuji, K., Asami, Y., Izawa, H., Shigenaga, A., et al. (2015). Molecular complex composed of β-cyclodextrin-grafted chitosan and pH-sensitive amphipathic peptide for enhancing cellular cholesterol efflux under acidic pH. *Bioconjugate Chemistry, 26*(3), 572–581.

53. Thews, O., Gassner, B., Kelleher, D. K., Schwerd, G., & Gekle, M. (2006). Impact of extracellular acidity on the activity of P-glycoprotein and the cytotoxicity of chemotherapeutic drugs. *Neoplasia, 8*(2), 143–152.